BMC Complementary Medicine and Therapies

RESEARCH

Open Access

# Ginsenoside Rg-1 prevents elevated cytosolic $Ca^{2+}$ via store-operated $Ca^{2+}$ entry in high-glucose–stimulated vascular endothelial and smooth muscle cells

A Young Han[1,2†], Su Min Ha[1†], You Kyoung Shin[1†] and Geun Hee Seol[1,3*]

## Abstract

**Background:** Ginsenoside Rg-1 (Rg-1), a triterpenoid saponin abundantly present in *Panax ginseng*, is a type of naturally occurring steroid with known anti-diabetic and anti-inflammatory effects. In this study, we sought to confirm the effects and mechanisms of action of Rg-1 on store-operated $Ca^{2+}$ entry (SOCE) in human vascular endothelial cell line (EA) and murine aortic vascular smooth muscle cell line (MOVAS) cells exposed to high glucose.

**Methods:** Cytosolic $Ca^{2+}$ concentrations in EA and MOVAS cells were measured by monitoring fluorescence of the ratiometric $Ca^{2+}$-indicator, Fura-2 AM.

**Results:** High glucose significantly increased $Ca^{2+}$ influx by abnormally activating SOCE in EA and MOVAS cells. Notably, this high glucose-induced increase in SOCE was restored to normal levels in EA and MOVAS cells by Rg-1. Moreover, Rg-1 induced reductions in SOCE in cells exposed to high glucose were significantly inhibited by the plasma membrane $Ca^{2+}$ ATPase (PMCA) blocker lanthanum, the $Na^+/K^+$-ATPase blocker ouabain, or the $Na^+/Ca^{2+}$ exchanger (NCX) blockers $Ni^{2+}$ and KB-R7943. These observations suggest that the mechanism of action of Rg-1 inhibition of SOCE involves PMCA and $Na^+/K^+$-ATPase, and an increase in $Ca^{2+}$ efflux via NCXs in both EA and MOVAS cells exposed to high glucose.

**Conclusions:** These findings indicate that Rg-1 may protect vascular endothelial and smooth muscle cells from $Ca^{2+}$ increases following exposure to hyperglycemic conditions.

**Keywords:** Ginsenoside Rg-1, Store-operated $Ca^{2+}$ entry, High glucose, Vascular endothelial cells, Vascular smooth muscle cells

## Background

$Ca^{2+}$, a second messenger involved in vast array of cellular processes such as metabolic signals, energy production, cell viability, and apoptosis [1]. $Ca^{2+}$ signals are generated by $Ca^{2+}$ influx from the extracellular space via plasma membrane $Ca^{2+}$ channels and through intracellular release from the endoplasmic reticulum (ER)/sarcoplasmic reticulum (SR) via $Ca^{2+}$-release channels [2]. Store-operated $Ca^{2+}$ entry (SOCE) is an important extracellular $Ca^{2+}$-influx mechanism in vascular endothelial

†A Young Han, Su Min Ha and You Kyoung Shin contributed equally to this work.

*Correspondence: ghseol@korea.ac.kr

[3] BK21 FOUR Program of Transdisciplinary Major in Learning Health Systems, Graduate School, Korea University, Seoul, Republic of Korea
Full list of author information is available at the end of the article

and smooth muscle cells [3]. In this mechanism, depletion of ER/SR $Ca^{2+}$ causes stromal interaction molecule 1 (STIM1) to bind to the ER-plasma membrane and signal the Orai channel to trigger $Ca^{2+}$ influx into the cytosol [4]. SOCE is critical to the primary $Ca^{2+}$ signaling pathway of cells and plays an essential role in a wide range of physiological functions, including extracellular excretion, enzyme activity, gene transcription, cell proliferation, and apoptosis [5].

High glucose causes an imbalance in cytosolic $Ca^{2+}$ homeostasis. High glucose upregulates STIM1 and increases Orai1 protein levels, thereby activating SOCE and increasing $Ca^{2+}$ influx [6, 7]. Previous studies have reported that STIM1 and Orai1 proteins are overexpressed in human aortic endothelial cells exposed to high glucose, resulting in increased $Ca^{2+}$ influx through SOCE [8], and have further shown that chronic exposure to high glucose significantly increases apoptosis in human umbilical vein endothelial cells owing to increased hydrogen peroxide production and SOCE-mediated activation of calcineurin [9]. Similar to what is observed in vascular endothelial cells, SOCE and Orai1 protein levels were significantly increased in human aortic smooth muscle cells exposed to high glucose [10].

$Ca^{2+}$ is intimately involved in the regulation of most cellular functions, such that even relatively small disturbances in $Ca^{2+}$ homeostasis can have fatal consequences for cellular function [11]. Disruption of $Ca^{2+}$ homeostasis causes vascular endothelial dysfunction by pathologically activating endothelial nitric oxide synthase [12] and increases the frequency of $Ca^{2+}$ spikes in vascular smooth muscle cells, leading to excessive vasoconstriction [13]. Therefore, an imbalance in cytosolic $Ca^{2+}$ homeostasis induced by high glucose is thought to have crucial effects on vascular health.

*Panax ginseng* is widely used in traditional herbal medicine owing to the pharmacological action of its ginsenoside saponins [14]. Among the 150 types of ginsenoside saponins, ginsenosides Rg-1 (Fig. 1), Rb-1 and Rg3 have demonstrated various pharmacological actions on cardiovascular, neuronal, and immune systems [15]. Moreover, ginsenosides are metformin mimetics with anti-diabetes properties [16]; among them, ginsenoside Rg-1 (hereafter, Rg-1) in particular, is known to have an excellent anti-diabetes profile. Rg-1 has also been demonstrated to directly protect pancreatic β-cell function and viability through the PI3K/Akt pathway [17]. Many studies have reported that Rg-1 not only inhibits the deterioration in the viability of cells exposed to high glucose, but also protect against cell damage. However, there are no reports of the effects of Rg-1 on SOCE or the underlying mechanism in vascular cells exposed to high glucose. Accordingly, we herein sought to investigate the preventive effects and related mechanisms of Rg-1 on SOCE in a human endothelial cell line (hereafter, EA) and a murine aortic vascular smooth muscle cell line (MOVAS) under high glucose.

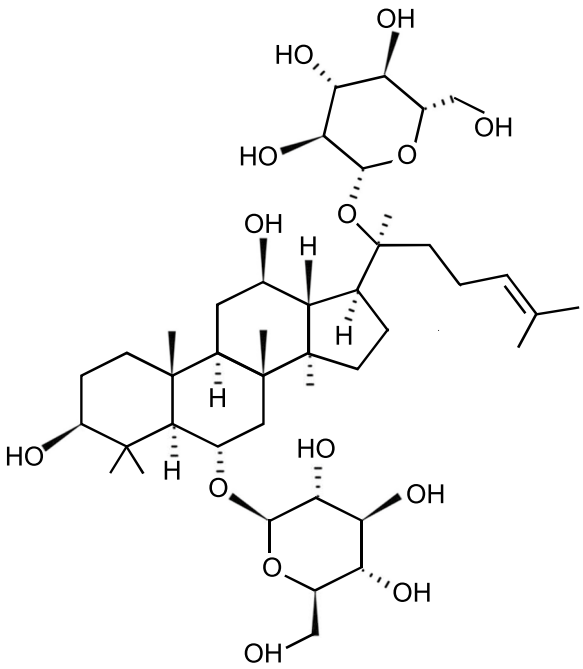


**Fig. 1** Molecular structure of ginsenoside Rg-1

## Methods

### Materials

Rg-1, Rb-1, glucose, lanthanum ($La^{3+}$), ouabain, nickel ($Ni^{2+}$) and KB-R7943 were purchased from Sigma-Aldrich (St. Louis, MO, USA). MTT (3-[4,5-dimethylthiazol-2-yl]-2,5 diphenyl tetrazolium bromide) solution was from Amresco (Solon, OH, USA), and Fura-2 AM was supplied by Molecular Probes (Eugene, OR, USA).

### Cell culture and hyperglycemia induction

EA cells, originally isolated from human umbilical veins, were purchased from the American Type Culture Collection (Manassas, VA, USA). MOVAS cells, isolated from aortic smooth muscle cells of C57BL6 mice, were purchased from Charles River Laboratories (Wilmington, MA, USA). EA and MOVAS cells were maintained in Dulbecco's modified Eagle's medium supplemented with 10% fetal bovine serum, 1% MEM non-essential amino acids, penicillin, and streptomycin. For culture under high-glucose conditions, cells were exposed to medium containing 30 mM glucose for 48 hours [18].

### Cell viability assay

The optimal concentration of Rg-1 was determined by first confirming cell viability using the MTT technique, according to the procedure described in a previous study [19]. Briefly, cells were seeded in 96-well plates at $1 \times 10^4$ cells per well in 200-μl aliquots. Cells were incubated with 0 to 50 μM Rg-1 at 37 °C for 48 hours. Each well was then washed with phosphate-buffered saline, followed by addition of a pure-grade MTT (5 mg/ml) solution to each well. After incubation for 3 hours, 100 ml dimethyl sulfoxide (DMSO) was added to each well to dissolve formazan crystals generated by reduction of MTT by metabolically active cells. Plates were incubated for an additional 3 hours in the dark, and the optical density of each well was measured at 540 nm using a plate reader (Spectrostar Nano; BMG LABTECH, Ortenberg, Germany).

### Cytosolic $Ca^{2+}$ measurement

EA and MOVAS cells were exposed to high glucose with or without Rg-1 for 48 hours. Cytosolic $Ca^{2+}$ was then measured using Fura-2 AM, a membrane-permeable, fluorescent ratiometric $Ca^{2+}$-binding dye [20]. Approximately $1 \times 10^6$/ml cells were incubated with 2.5 μM Fura-2 AM in the dark for 30 minutes at room temperature. Dye remaining in the extracellular fluid was removed by exchanging the supernatant twice. Cells were placed in a quartz cuvette, and fluorescence at 510 nm was measured using a fluorescence spectrometer (Photon Technology Instruments) with alternating wavelengths of 340 nm and 380 nm with a chopper wheel (50 Hz). Cytosolic $Ca^{2+}$ was expressed as the ratio of fluorescence at 340 nm to fluorescence at 380 nm (F340/F380).

### Data analysis and statistics

All statistical analyses were performed using SPSS Statistics software version 26 (IBM, IL, USA). Data are expressed as means ± standard error of the mean (SEM). Differences among groups were analyzed by analysis of variance and Fisher's Least Significant Difference post-hoc test. $p$-values $< 0.05$ were considered statistically significant.

## Results

### Effects of ginsenosides Rg-1 and Rb-1 on high-glucose–exposed EA and MOVAS cells

First, we compared the effects of Rg-1 and Rb-1 on SOCE in EA and MOVAS cells exposed to high glucose. In the normal glucose group, the effects of Rg-1 and Rb-1 on SOCE did not significantly differ between EA and MOVAS cell. However, the SOCE-inhibitory effects of Rg-1 and Rb-1 were different in the high-glucose group, with Rg-1 significantly reducing SOCE in both EA and MOVAS cells and Rb-1 significantly decreasing SOCE only in MOVAS cells (Fig. 2A-C). These findings confirmed that, of the ginsenosides evaluated, Rg-1 had a greater effect than Rb-1 on $Ca^{2+}$ homeostasis in EA and MOVAS cells exposed to high glucose.

### Optimal Rg-1 concentration inhibiting SOCE in high-glucose–exposed EA and MOVAS cells

The optimal Rg-1 concentration inhibiting SOCE was determined by the MTT method. Incubation of EA and MOVAS cells with 0, 0.01, 0.1, 1, 10, 20 or 50 μM Rg-1 showed that Rg-1 at concentrations above 20 μM significantly reduced cell viability compared with controls (data not shown). In addition, the effect of Rg-1 on the degree of SOCE inhibition was assessed by incubating EA and MOVAS cells exposed to high glucose with 0.1, 1, or 10 μM Rg-1. In both cell types, 10 μM Rg-1 concentration significantly reduced the high glucose-induced increase in SOCE, restoring normal glucose levels, whereas neither 0.1 nor 1 μM Rg-1 had any effect (Fig. 3A-C). Thus, Rg-1 was used at a concentration of 10 μM in subsequent experiments.

### Mechanisms of SOCE inhibition by ginsenoside Rg-1 on high-glucose–exposed EA and MOVAS cells

The mechanism of SOCE inhibition by Rg-1 was analyzed by comparing its effect with the effects of the plasma membrane $Ca^{2+}$ ATPase (PMCA) blocker $La^{3+}$; the $Na^+/K^+$ ATPase blocker ouabain; and the $Na^+/Ca^{2+}$ exchanger (NCX) blockers, $Ni^{2+}$ and KB-R7943. Specifically, KB-R7943 is an inhibitor of the reverse mode of $Na^+/Ca2^+$ exchanger.

SOCE was more substantially inhibited in cells pretreated with $La^{3+}$ plus Rg-1 compared with cells pretreated with $La^{3+}$ alone. $La^{3+}$ alone significantly decreased SOCE in high-glucose–exposed EA cells, but not MOVAS cells. Notably, $La^{3+}$ plus Rg-1 resulted in a significantly greater increase in SOCE than Rg-1 alone in both EA and MOVAS cells exposed to high glucose (Fig. 4A-C). These results suggest that the mechanism by which Rg-1 decreases SOCE in EA and MOVAS cells exposed to high glucose may be associated with the PMCA pathway.

To determine whether the SOCE inhibitory effect of Rg-1 was related to $Na^+/K^+$ channels, EA and MOVAS cells exposed to high glucose were pretreated with Rg-1, the $Na^+/K^+$ ATPase blocker ouabain, or both. Treatment of cells exposed to high glucose with ouabain or Rg-1 alone reduced SOCE compared with controls. Compared with Rg-1 alone, however, Rg-1 plus ouabain significantly increased SOCE (Fig. 5A-C). This suggests that Rg-1 increases $Ca^{2+}$ efflux in EA and MOVAS cells exposed to high glucose via the $Na^+/K^+$ ATPase pathway.

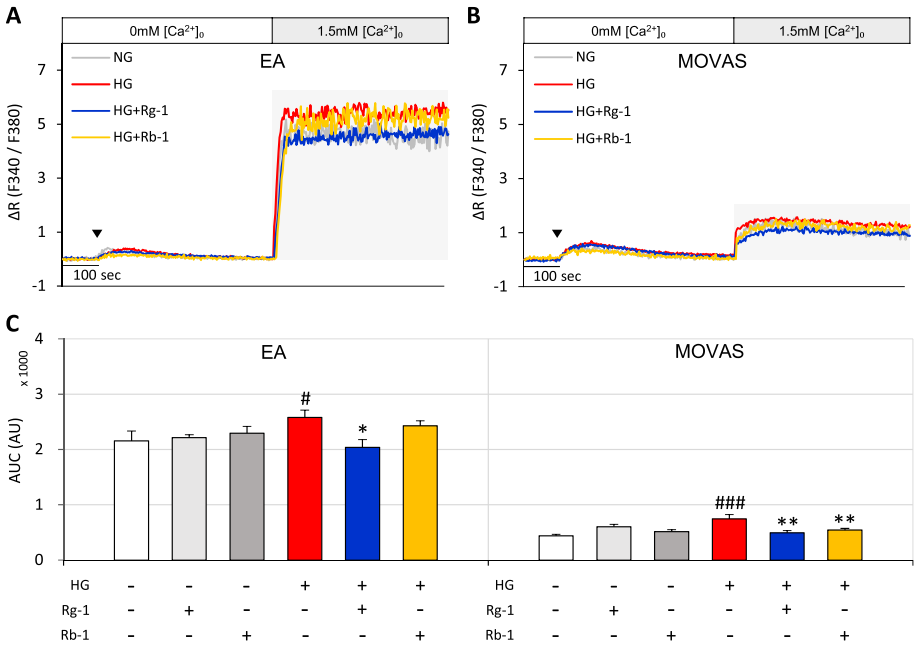


**Fig. 2** Effects of Rg-1 on SOCE in EA and MOVAS cells exposed to high glucose compared with those of Rb-1. **A** Representative traces showing the effects of normal glucose, high glucose, and high glucose with 10 μM Rg-1 or 10 μM Rb-1, on SOCE in EA cells. **B** Representative traces showing the effects of normal glucose, high glucose, and high glucose with 10 μM Rg-1 or 10 μM Rb-1, on SOCE in MOVAS cells. **C** Summary data showing area under the curve (AUC) values for 500 seconds for EA and MOVAS cells. Data are means ± SEM ($n = 6–14$; $^{\#}p < 0.05$, $^{\#\#\#}p < 0.001$ compared with normal glucose; $^{*}p < 0.05$, $^{**}p < 0.01$ compared with high glucose). The symbol (▼) indicates the time point at which 30 μM BHQ was applied

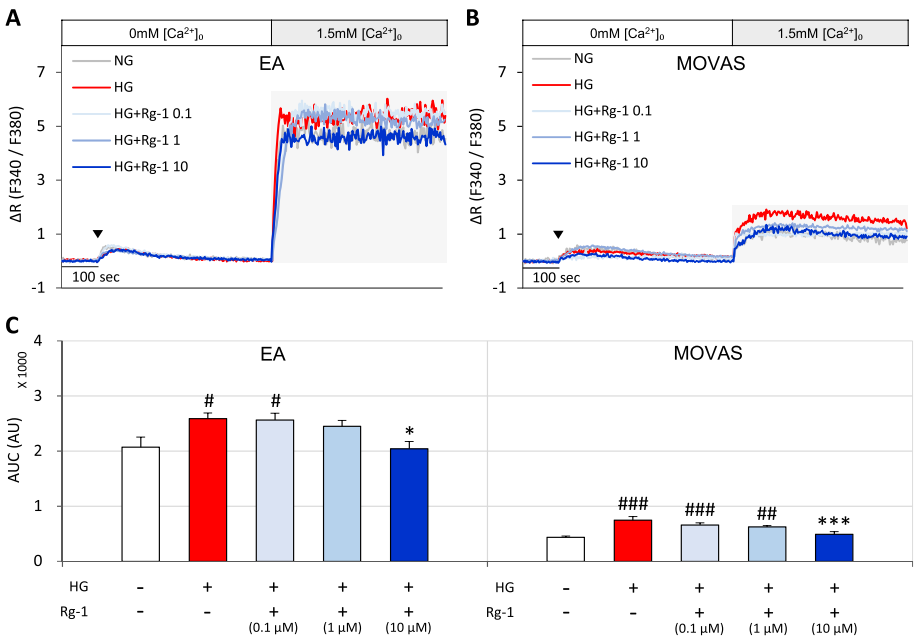


**Fig. 3** Effects of various concentrations of Rg-1 on SOCE in EA and MOVAS cells exposed to high glucose. **A** & **B** Representative traces showing effects of normal glucose, high glucose, and high glucose plus 0.1, 1, or 10 μM Rg-1 on SOCE in **(A)** EA cells and (**B)** MOVAS cells. **C** Summary data showing area under the curve (AUC) values for 500 seconds for EA and MOVAS cells. The symbol (▼) indicates the time point at which 30 μM BHQ was applied. Data are means ± SEM ($n = 6–11$; $^{\#}p < 0.05$, $^{\#\#}p < 0.01$, $^{\#\#\#}p < 0.001$ compared with normal glucose; $^{*}p < 0.05$, $^{***}p < 0.001$ compared with high glucose)

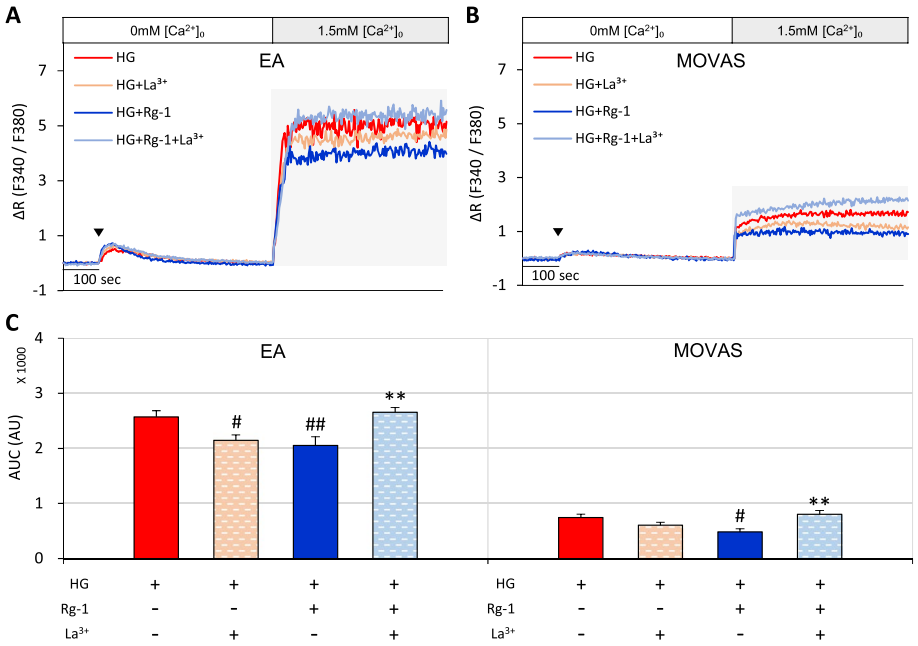


**Fig. 4** Effects of $La^{3+}$ on Rg-1–induced increases in SOCE in EA and MOVAS cells exposed to high glucose. **A** & **B** Representative traces showing the effects of high glucose, high glucose plus 125 μM $La^{3+}$, high glucose plus 10 μM Rg-1, and high glucose plus 10 μM Rg-1 and 125 μM $La^{3+}$ on SOCE in (**A)** EA and (**B)** MOVAS cells. **C** Summary data showing area under the curve (AUC) values for 500 seconds for EA and MOVAS cells. The symbol (▼) indicates the time point at which 30 μM BHQ was applied. Data are means ± SEM ($n = 7–11$; $^{\#}p < 0.05$, $^{\#\#}p < 0.01$ compared with high glucose; $^{**}p < 0.01$ compared with high glucose plus Rg-1)

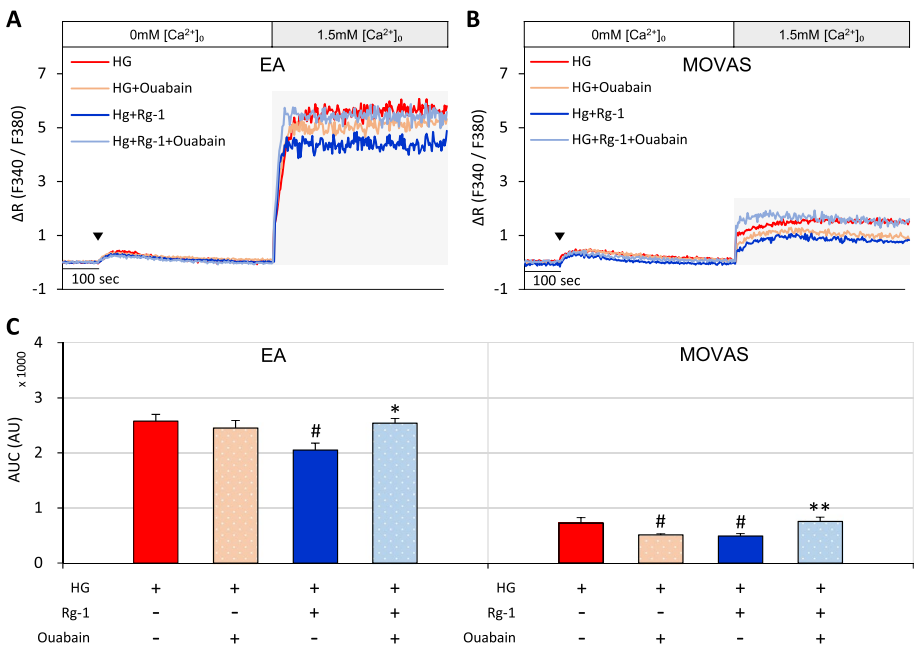


**Fig. 5** Effects of ouabain on Rg-1–induced increases in SOCE in EA and MOVAS cells exposed to high glucose. **A** & **B** Representative traces showing the effects of high glucose, high glucose plus 10 nM ouabain, high glucose plus 10 μM Rg-1, and high glucose plus 10 μM Rg-1 and 10 nM ouabain on SOCE in (**A)** EA and (**B)** MOVAS cells. **C** Summary data showing area under the curve (AUC) values for 500 seconds for EA and MOVAS cells. The symbol (▼) indicates the time point at which 30 μM BHQ was applied. Data are means ± SEM ($n = 6–11$; $^{\#}p < 0.05$ compared with high glucose; $^{*}p < 0.05$, $^{**}p < 0.01$ compared with high glucose plus Rg-1)

The NCX pathway has been reported to be effective in coping with increased intracellular $Ca^{2+}$ in pancreatic cells [21]. Therefore, we assessed whether the Rg-1-induced reduction in SOCE was related to the NCX pathway. Treatment of EA and MOVAS cells with $Ni^{2+}$ or KB-R7943 inhibited the high glucose-induced increase in SOCE to a level similar to that of Rg-1. However, SOCE was more substantially increased in cells pretreated with Rg-1 plus $Ni^{2+}$ or Rg-1 plus KB-R7943 than in cells pretreated with $Ni^{2+}$ or KB-R7943 alone, respectively (Fig. 6A-C).

Collectively, these findings indicate that high glucose significantly increases $Ca^{2+}$ influx by abnormally activating SOCE in EA and MOVAS cells, and that Rg-1 reverses SOCE by increasing $Ca^{2+}$ efflux through PMCA, $Na^{+}/K^{+}$ ATPase, and NCX.

## Discussion

In vascular endothelial and smooth muscle cells, the SOCE pathway, activated by depletion of intracellular $Ca^{2+}$ stores, plays an important role in regulating intracellular functions [3]. High glucose exposure promotes enhanced permeability and proliferation of human coronary artery endothelial cells through increases in SOCE via Orai-mediated, $Ca^{2+}$ release-activated $Ca^{2+}$ channels [22]. Notably in this context, it has been reported that diabetic hyperglycemia increases the expression of Orai1 and SOCE in vascular smooth muscle cells [10]. Our findings demonstrated that exposure to high glucose resulted in a significant increase in SOCE in EA and MOVAS cells; this effect was inhibited by Rg-1 treatment, which restored $Ca^{2+}$ to levels found under normal glucose conditions; this Rg-1-associated inhibition of SOCE in EA and MOVAS cells exposed to high glucose might be related to the PMCA, $Na^{+/}K^{+}$ ATPase, and NCX pathways (Fig. 7). Notably, Rg-1 did not have a significant SOCE-inhibitory effect under normoglycemic conditions, but only exhibited this action under hyperglycemic conditions. In a similar vein, a study investigating the blood pressure effects of *Codonopsis lanceolata*, a natural plant rich in triterpenoid saponins, showed no effect on blood pressure in the normotensive group, but exerted a significant blood pressure-lowering effect in the hypertensive group [23].

In this study, treatment with $Ca^{2+}$ antagonists such as $La^{3+}$, ouabain, $Ni^{2+}$, and KB-R7943 reduced SOCE in cells exposed to high glucose concentrations. However, incubation of cells with both Rg-1 and $Ca^{2+}$ antagonists resulted in a rapid increase in SOCE. Increased intracellular $Ca^{2+}$ is returned to the extracellular compartment

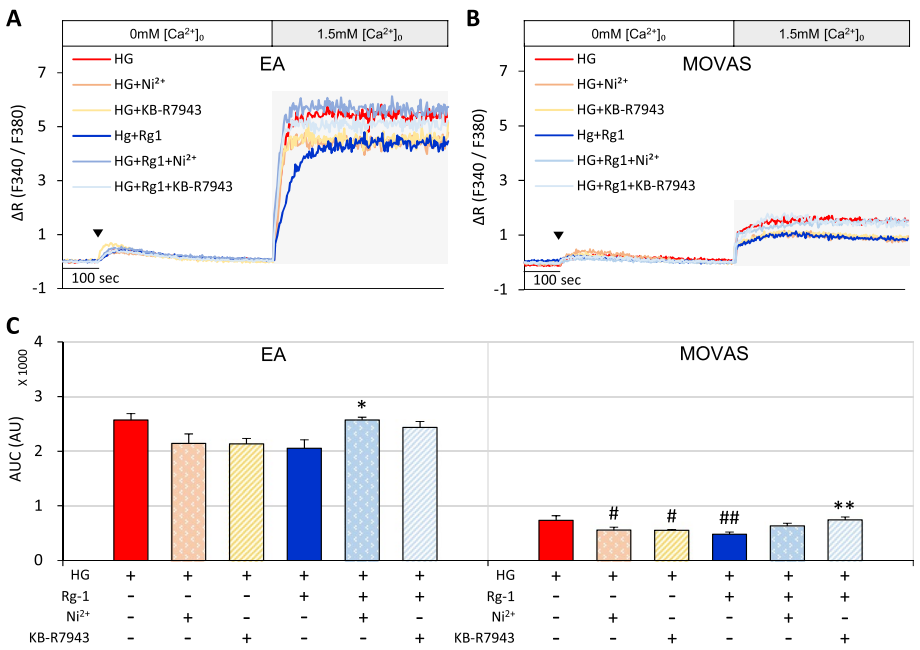


**Fig. 6** Effects of $Ni^{2+}$ and KB-R7943 on Rg-1–induced increases in SOCE in EA and MOVAS cells exposed to high glucose. **A** & **B** Representative traces showing the effects of high glucose, high glucose plus 100 nM $Ni^{2+}$, high glucose plus 10 μM KB-R7943, high glucose plus 10 μM Rg-1, high glucose plus 10 μM Rg-1 and 100 nM $Ni^{2+}$, and high glucose plus 10 μM Rg-1 and 10 μM KB-R7943 on SOCE in (**A**) EA and (**B**) MOVAS cells. **C** Summary data showing area under the curve (AUC) values for 500 seconds for EA and MOVAS cells. The symbol (▼) indicates the time point at which 30 μM BHQ was applied. Data are means ± SEM ($n = 6$–12; $^{\#}p < 0.05$, $^{\#\#}p < 0.01$ compared with high glucose; $^{*}p < 0.05$, $^{**}p < 0.01$ compared with high glucose plus Rg-1)

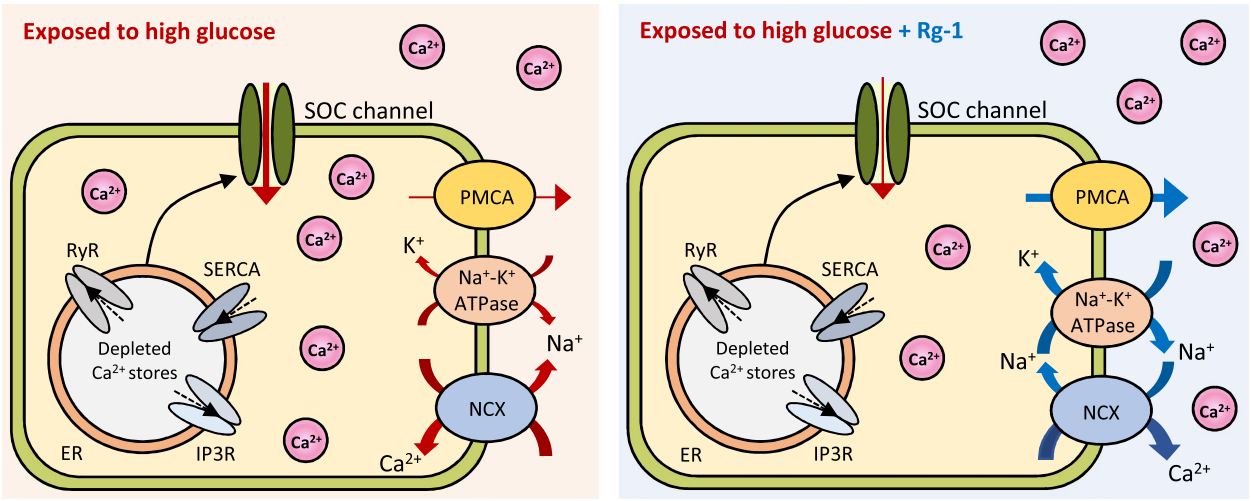


**Fig. 7** Action mechanisms of Rg-1 on SOCE in EA and MOVAS cells exposed to high glucose. The red and blue colors indicate changes in the regulation of intracellular $Ca^{2+}$ levels by exposure to high glucose or Rg-1 treatment, respectively. The thicknesses of the arrows reflect the amount of $Ca^{2+}$ influx or efflux

by the action of the PMCA: This was shown, for example, by treatment of cells with 125 μM $La^{3+}$, which blocked PMCA [24]. Treatment of pancreatic beta cells with 22.2 mM glucose resulted in significantly greater reductions in PMCA1 and PMCA2 mRNAs than treatment with 2.8 mM glucose [25]. These findings, showing that PMCA activity was inhibited under high glucose conditions, suggest that the inhibition of PMCA may have affected the increase in SOCE under high glucose than normal glucose conditions. In addition, the inhibition of SOCE by a relatively high concentration of $La^{3+}$ under high glucose conditions may be due to its blocking of non-selective cation channels. Conversely, the increase in SOCE induced by treatment with both $La^{3+}$ and Rg-1 under high glucose conditions may be related to the Rg-1-induced increase of $Ca^{2+}$ efflux through PMCA, which inhibits SOCE under high glucose conditions.

Exposure of pancreatic β-cells to glucose leads to conversion of a PMCA-based, low-efficiency $Ca^{2+}$ efflux mechanism to an NCX-based, high-efficiency system that is better able to cope with glucose-induced $Ca^{2+}$ influx [21]. As the glycemic load in pancreatic β-cells increases, it induces a concentration-dependent decrease in PMCA activity, while significantly increasing NCX activity [25]. NCX is a reversible transporter of $Ca^{2+}$ across plasma membranes. Exposure to abnormally high glucose concentrations has been reported to increase NCX activity and contribute to diabetic microvascular complications [26, 27]. This increase in NCX activity was inhibited by KB-R7943, suggesting that hyperglycemia-induced NCX activity is strongly associated with the NCX reverse mode [28]. In the present study, Rg-1 treatment inhibited the abnormally increased SOCE induced by high glucose concentrations, suggesting that Rg-1 may inhibit $Ca^{2+}$ influx through the NCX reverse mode. In contrast, treatment with both Rg-1 and KB-R7943 under high glucose conditions resulted in a greater increase in SOCE than high glucose alone. Because pretreatment with KB-R7943 was found to increase the intracellular basal sodium concentration in cardiomyocytes of diabetic rats [27], the increased potential difference may depolarize cells and stimulate voltage-dependent calcium channels. When $Ca^{2+}$ influx is excessively disturbed, various ion channels, such as NCXs or voltage-operated $Ca^{2+}$ channels, play an important role in generating the $Ca^{2+}$ influx underlying oscillations [29–31]. Future studies needed to assess the effects of Rg-1 on the expression of $Ca^{2+}$ channel proteins, especially the expression of proteins that regulate SOCE, such as Orai1, Orai2, Orai3, STIM1, and STIM2.

Hyperglycemia-induced metabolic dysfunctions, such as enhanced formation of advanced glycation end products (AGEs) and increased production of reactive oxygen species, have been suggested as factors for developing diabetic vascular complications [32]. In mouse mesangial cells, high glucose enhanced the formation of methylglyoxal (the major precursor of AGEs) and the level of 8-OHdG, suggesting increased oxidative stress [33]. In line with these reports, catalase treatment of platelets from patients with type 2 diabetes mellitus increased the PMCA tyrosine phosphorylation induced by thapsigargin plus ionomycin, suggesting that oxidative stress is involved in the reduced platelet PMCA activity seen in diabetic patients [34]. High glucose also significantly increased NCX activity and

malondialdehyde production in human umbilical vascular endothelial cells, and this effect was abolished by KB-R7943-mediated inhibition of the reverse mode of NCX, indicating that increased reverse-mode NCX activity plays an important role in high glucose-induced endothelial dysfunction [28]. Rg-1 has demonstrated several pharmacological actions including antioxidant effects [35]. Rg-1 reduces reactive oxygen species (ROS) by modulating Nrf2 (nuclear factor-erythrocyte 2-related factor 2) and NLRP3 (nucleotide-binding oligomerization domain-like receptor protein 3) signaling pathways [36]. Several studies have shown that hyperglycemia induces lipid peroxidation, nitrite production, and intracellular ROS formation [37, 38]. In the current study, the reduction in SOCE is probably related to the antioxidant activity of Rg-1.

In vascular endothelial cells, Rg-1 produced a more prominent SOCE-reducing effect than Rb-1. Although few studies have investigated the regulation of intracellular $Ca^{2+}$ in vascular cells by Rb-1, one study in rat cortical synaptosomes showed that it decreased intracellular $Ca^{2+}$ by increasing $Na^{+}/K^{+}$-ATPase and $Ca^{2+}/Mg^{2+}$-ATPase activity [39]. In addition, Rb-1 protects cardiomyocytes by reducing the high-$Ca^{2+}$–induced delayed afterdepolarizations of cardiomyocytes. On the other hand, Rg-1 has been reported to have $Ca^{2+}$-regulating effects in various cell types. In an ischemia-reperfused hippocampal cell model, it was shown to have neuroprotective effects by blocking excess $Ca^{2+}$ influx and decreasing neuronal nitric oxide synthase activity [40]. In myocardial cells, it has been shown that, Rg-1 restores cellular homeostasis by reducing ROS and inhibiting $Ca^{2+}$ influx [41]. In neurons, Rg-1 shows a cell-protective effect through a reduction in intracellular free $Ca^{2+}$ [42] and exerts a $Ca^{2+}$ homeostasis-maintenance effect by reducing ROS and oxidative stress and protecting against neuroinflammation [43]. In lymphocytes, Rg-1 has been shown to inhibit $Ca^{2+}$ influx attributable to $H_2O_2$-induced damage and significantly reduce apoptosis and lymphocyte damage caused by oxidative stress, indicating protective effects on immune cells [44]. Therefore, Rg-1 exerts cytoprotective effects under pathological conditions by maintaining $Ca^{2+}$ homeostasis. However, further studies are needed to show the different mechanism of Rg-1 in different cell types such as endothelial cell and smooth muscle cells.

## Conclusions

Present study demonstrated that treatment with Rg-1 may be a new approach to protecting vascular endothelial and smooth muscle cells in patients with hyperglycemia through maintenance of $Ca^{2+}$ homeostasis.

### Abbreviations

AGE: Advanced glycation end product; AUC: Area under the curve; DMSO: Dimethyl sulfoxide; EA: Human endothelial cell line; ER: Endoplasmic reticulum; MOVAS: Murine aortic vascular smooth muscle cell line; NCX: $Na^{+}/Ca^{2+}$ exchanger; PMCA: Plasma membrane $Ca^{2+}$ ATPase; SEM: Standard error of the mean; SOCE: Store-operated $Ca^{2+}$ entry; SR: Sarcoplasmic reticulum; STIM: Stromal interaction molecule; ROS: Reactive oxygen species.

### Acknowledgements

Not applicable.

### Authors' contributions

Conceptualization, G.H.S.; methodology, G.H.S.; formal analysis, A.Y.H., S.M.H., Y.K.S. and G.H.S.; funding acquisition, G.H.S.; investigation, A.Y.H., S.M.H. and Y.K.S.; project administration, G.H.S.; supervision, G.H.S.; writing—original draft preparation, A.Y.H., S.M.H., Y.K.S. and G.H.S.; writing—review and editing, G.H.S.; visualization, A.Y.H. and G.H.S. All authors have read and approved the final manuscript.

### Funding

This work was supported by a grant from the Basic Science Research Program through the National Research Foundation of Korea (NRF-2021R1A2C2004118, 2020R1I1A1A0107450513) and the Institute of Nursing Research, Korea University Grant. This manuscript is a revision of SMH's master's thesis from Korea University.

### Availability of data and materials

All data generated or analyzed during this study are included in this published article.

## Declarations

### Ethics approval and consent to participate

Not applicable.

### Consent for publication

Not applicable.

### Competing interests

The authors declare that they have no competing interests.

### Author details

[1]Department of Basic Nursing Science, College of Nursing, Korea University, 145 Anam-ro, Seongbuk-gu, Seoul 02841, Republic of Korea. [2]Department of Nursing, College of Life Science and Industry, Sunchon National University, Suncheon, Republic of Korea. [3]BK21 FOUR Program of Transdisciplinary Major in Learning Health Systems, Graduate School, Korea University, Seoul, Republic of Korea.

Received: 10 May 2022 Accepted: 10 June 2022
Published online: 22 June 2022

### References

1. Marchi S, Patergnani S, Missiroli S, Morciano G, Rimessi A, Wieckowski MR, et al. Mitochondrial and endoplasmic reticulum calcium homeostasis and cell death. Cell Calcium. 2018;69:62–72. https://doi.org/10.1016/j.ceca.2017.05.003.
2. Hogan PG, Rao A. Store-operated calcium entry: mechanisms and modulation. Biochem Biophys Res Commun. 2015;460:40–9. https://doi.org/10.1016/j.bbrc.2015.02.110.
3. Avila-Medina J, Mayoral-González I, Galeano-Otero I, Redondo PC, Rosado JA, Smani T. Pathophysiological significance of store-operated calcium entry in cardiovascular and skeletal muscle disorders and angiogenesis. Adv Exp Med Biol. 2020;1131:489–504. https://doi.org/10.1007/978-3-030-12457-1_19.
4. Shen Y, Thillaiappan NB, Taylor CW. The store-operated Ca2+ entry complex comprises a small cluster of STIM1 associated with one Orai1

channel. Proc Natl Acad Sci U S A. 2021;118:e2010789118. https://doi.org/10.1073/pnas.2010789118.
5. Parekh AB, Putney JW Jr. Store-operated calcium channels. Physiol Rev. 2005;85:757–810. https://doi.org/10.1152/physrev.00057.2003.
6. Chaudhari S, Wu P, Wang Y, Ding Y, Yuan J, Begg M, et al. High glucose and diabetes enhanced store-operated Ca2+ entry and increased expression of its signaling proteins in mesangial cells. Am J Physiol Renal Physiol. 2014;306:F1069–F80. https://doi.org/10.1152/ajprenal.00463.2013.
7. Xu Z, Xu W, Song Y, Zhang B, Li F, Liu Y. Blockade of store-operated calcium entry alleviates high glucose-induced neurotoxicity via inhibiting apoptosis in rat neurons. Chem Biol Interact. 2016;254:63–72. https://doi.org/10.1016/j.cbi.2016.05.025.
8. Daskoulidou N, Zeng B, Berglund LM, Jiang H, Chen G-L, Kotova O, et al. High glucose enhances store-operated calcium entry by upregulating ORAI/STIM via calcineurin-NFAT signalling. J Mol Med. 2015;93:511–21. https://doi.org/10.1007/s00109-014-1234-2.
9. Tamareille S, Mignen O, Capiod T, Rücker-Martin C, Feuvray D. High glucose-induced apoptosis through store-operated calcium entry and calcineurin in human umbilical vein endothelial cells. Cell Calcium. 2006;39:47–55. https://doi.org/10.1016/j.ceca.2005.09.008.
10. Ma K, Sukkar B, Zhu X, Zhou K, Cao H, Voelkl J, et al. Stimulation of ORAI1 expression, store-operated Ca2+ entry, and osteogenic signaling by high glucose exposure of human aortic smooth muscle cells. Pflug Arch Eur J Physiol. 2020;472:1093–102. https://doi.org/10.1007/s00424-020-02405-1.
11. Petersen OH, Michalak M, Verkhratsky A. Calcium signalling: past, present and future. Cell Calcium. 2005;38:161–9. https://doi.org/10.1016/j.ceca.2005.06.023.
12. Goligorsky MS. Vascular endothelium in diabetes. Am J Physiol Renal Physiol. 2017;312:F266–F75. https://doi.org/10.1152/ajprenal.00473.2016.
13. Navedo MF, Takeda Y, Nieves-Cintrón M, Molkentin JD, Santana LF. Elevated Ca2+ sparklet activity during acute hyperglycemia and diabetes in cerebral arterial smooth muscle cells. Am J Physiol Cell Physiol. 2010;298:C211–C20. https://doi.org/10.1152/ajpcell.00267.2009.
14. Yu T, Yang Y, Kwak Y-S, Song GG, Kim M-Y, Rhee MH, et al. Ginsenoside Rc from Panax ginseng exerts anti-inflammatory activity by targeting TANK-binding kinase 1/interferon regulatory factor-3 and p38/ATF-2. J Ginseng Res. 2017;41:127–33. https://doi.org/10.1016/j.jgr.2016.02.001.
15. Mohanan P, Subramaniyam S, Mathiyalagan R, Yang D-C. Molecular signaling of ginsenosides Rb1, Rg1, and Rg3 and their mode of actions. J Ginseng Res. 2018;42:123–32. https://doi.org/10.1016/j.jgr.2017.01.008.
16. Aliper A, Jellen L, Cortese F, Artemov A, Karpinsky-Semper D, Moskalev A, et al. Towards natural mimetics of metformin and rapamycin. Aging (Albany NY). 2017;9:2245–68. https://doi.org/10.18632/aging.101319.
17. Li N, Zhang H, Li X. Ginsenoside Rg1 protects pancreatic INS-1 cell survival in β-cell through the PI3K/Akt signaling pathway. Metab Clin Exp. 2020;104:154078. https://doi.org/10.1016/j.metabol.2019.12.024.
18. Zhang R-J, Hao H-Y, Liu Q-J, Zuo H-Y, Chang Y-N, Zhi Z-J, et al. Protective effects of Schisandrin on high glucose-induced changes of RhoA and eNOS activity in human umbilical vein endothelial cells. Pathol Res Pract. 2018;214:1324–9. https://doi.org/10.1016/j.prp.2018.02.010.
19. Han AY, Lee HS, Seol GH. Foeniculum vulgare mill. Increases cytosolic Ca2+ concentration and inhibits store-operated Ca2+ entry in vascular endothelial cells. Biomed Pharmacother. 2016;84:800–5. https://doi.org/10.1016/j.biopha.2016.10.013.
20. Kim MK, Han AY, Shin YK, Lee K-W, Seol GH. Codonopsis lanceolata contributes to Ca2+ homeostasis by mediating SOCE and PLC/IP3 pathways in vascular endothelial and smooth muscle cells. Planta Med. 2020;86:1345–52. https://doi.org/10.1055/a-1214-6718.
21. Herchuelz A, Kamagate A, Ximenes H, Van Eylen F. Role of Na/ca exchange and the plasma membrane Ca2+—ATPase in β cell function and death. Ann N Y Acad Sci. 2007;1099:456–67. https://doi.org/10.1196/annals.1387.048.
22. Bai S, Wei Y, Hou W, Yao Y, Zhu J, Hu X, et al. Orai-IGFBP3 signaling complex regulates high-glucose exposure-induced increased proliferation, permeability, and migration of human coronary artery endothelial cells. BMJ Open Diabetes Res Care. 2020;8:e001400. https://doi.org/10.1136/bmjdrc-2020-001400.
23. Han AY, Lee YS, Kwon S, Lee HS, Lee K-W, Seol GH. Codonopsis lanceolata extract prevents hypertension in rats. Phytomedicine. 2018;39:119–24. https://doi.org/10.1016/j.phymed.2017.12.028.
24. Chen J, McLean PA, Neel BG, Okunade G, Shull GE, Wortis HH. CD22 attenuates calcium signaling by potentiating plasma membrane calcium-ATPase activity. Nat Immunol. 2004;5:651–7. https://doi.org/10.1038/ni1072.
25. Ximenes HM, Kamagate A, Van Eylen F, Carpinelli A, Herchuelz A. Opposite effects of glucose on plasma membrane Ca2+—ATPase and Na/ca exchanger transcription, expression, and activity in rat pancreatic β-cells. J Biol Chem. 2003;278:22956–63. https://doi.org/10.1074/jbc.M212339200.
26. Li J, Jin H-B, Sun Y-M, Su Y, Wang L-F. KB-R7943 inhibits high glucose-induced endothelial ICAM-1 expression and monocyte-endothelial adhesion. Biochem Biophys Res Commun. 2010;392:516–9. https://doi.org/10.1016/j.bbrc.2009.12.183.
27. Nishio S, Teshima Y, Takahashi N, Thuc LC, Saito S, Fukui A, et al. Activation of CaMKII as a key regulator of reactive oxygen species production in diabetic rat heart. J Mol Cell Cardiol. 2012;52:1103–11. https://doi.org/10.1016/j.yjmcc.2012.02.006.
28. Liu D, Cui K-Z, Sun Y-M, Liu J-W, Li Y-B, Su Y. Protective effects of the sodium/calcium exchanger inhibitor on endothelial dysfunction induced by high glucose. Exp Clin Endocrinol Diabete. 2015;123:7–10. https://doi.org/10.1055/s-0034-1385924.
29. Country MW, Campbell BF, Jonz MG. Spontaneous action potentials in retinal horizontal cells of goldfish (Carassius auratus) are dependent upon L-type Ca2+ channels and ryanodine receptors. J Neurophysiol. 2019;122:2284–93. https://doi.org/10.1152/jn.00240.2019.
30. Fodor J, Matta C, Oláh T, Juhász T, Takács R, Tóth A, et al. Store-operated calcium entry and calcium influx via voltage-operated calcium channels regulate intracellular calcium oscillations in chondrogenic cells. Cell Calcium. 2013;54:1–16. https://doi.org/10.1016/j.ceca.2013.03.003.
31. Luo L, Song S, Ezenwukwa CC, Jalali S, Sun B, Sun D. Ion channels and transporters in microglial function in physiology and brain diseases. Neurochem Int. 2021;142:104925. https://doi.org/10.1016/j.neuint.2020.104925.
32. Yamagishi S-i, Maeda S, Matsui T, Ueda S, Fukami K, Okuda S. Role of advanced glycation end products (AGEs) and oxidative stress in vascular complications in diabetes. Biochim Biophys Acta. 2012;1820:663–71. https://doi.org/10.1016/j.bbagen.2011.03.014.
33. Kim KM, Kim YS, Jung DH, Lee J, Kim JS. Increased glyoxalase I levels inhibit accumulation of oxidative stress and an advanced glycation end product in mouse mesangial cells cultured in high glucose. Exp Cell Res. 2012;318:152–9. https://doi.org/10.1016/j.yexcr.2011.10.013.
34. Jardin I, Redondo PC, Salido GM, Pariente JA, Rosado JA. Endogenously generated reactive oxygen species reduce PMCA activity in platelets from patients with non-insulin-dependent diabetes mellitus. Platelets. 2006;17:283–8. https://doi.org/10.1080/09537100600745187.
35. Gao Y, Li J, Wang J, Li X, Li J, Chu S, et al. Ginsenoside Rg1 prevent and treat inflammatory diseases: a review. Int Immunopharmacol. 2020;87:106805. https://doi.org/10.1016/j.intimp.2020.106805.
36. Gao Y, Li J, Chu S, Zhang Z, Chen N, Li L, et al. Ginsenoside Rg1 protects mice against streptozotocin-induced type 1 diabetic by modulating the NLRP3 and Keap1/Nrf2/HO-1 pathways. Eur J Pharmacol. 2020;866:172801. https://doi.org/10.1016/j.ejphar.2019.172801.
37. Jayakumar T, Chang C-C, Lin S-L, Huang Y-K, Hu C-M, Elizebeth AR, et al. Brazilin ameliorates high glucose-induced vascular inflammation via inhibiting ROS and CAMs production in human umbilical vein endothelial cells. Biomed Res Int. 2014;2014:403703. https://doi.org/10.1155/2014/403703.
38. Zhuang X, Maimaitijiang A, Li Y, Shi H, Jiang X. Salidroside inhibits high-glucose induced proliferation of vascular smooth muscle cells via inhibiting mitochondrial fission and oxidative stress. Exp Ther Med. 2017;14:515–24. https://doi.org/10.3892/etm.2017.4541.
39. Jiang X, Zhang J, Shi C. Mechanism of action of ginsenoside Rb1 in decreasing intracellular Ca2+. Acta Pharm Sin. 1996;31:321–6.
40. He Q, Sun J, Wang Q, Wang W, He B. Neuroprotective effects of ginsenoside Rg1 against oxygen–glucose deprivation in cultured hippocampal neurons. J Chin Med Assoc. 2014;77:142–9. https://doi.org/10.1016/j.jcma.2014.01.001.
41. Zhu D, Wu L, Li CR, Wang XW, Ma YJ, Zy Z, et al. Ginsenoside Rg1 protects rat cardiomyocyte from hypoxia/reoxygenation oxidative injury via antioxidant and intracellular calcium homeostasis. J Cell Biochem. 2009;108:117–24. https://doi.org/10.1002/jcb.22233.

42. Zhang Y-F, Fan X-J, Li X, Peng L-L, Wang G-H, Ke K-F, et al. Ginsenoside Rg1 protects neurons from hypoxic–ischemic injury possibly by inhibiting Ca2+ influx through NMDA receptors and L-type voltage-dependent Ca2+ channels. Eur J Pharmacol. 2008;586:90–9. https://doi.org/10.1016/j.ejphar.2007.12.037.
43. Han Y, Li X, Yang L, Zhang D, Li L, Dong X, et al. Ginsenoside Rg1 attenuates cerebral ischemia-reperfusion injury due to inhibition of NOX2-mediated calcium homeostasis dysregulation in mice. J Ginseng Res. 2021;46:515–25. https://doi.org/10.1016/j.jgr.2021.08.001.
44. Bi S, Ma X, Wang Y, Chi X, Zhang Y, Xu W, et al. Protective effect of ginsenoside Rg1 on oxidative damage induced by hydrogen peroxide in chicken splenic lymphocytes. Oxidative Med Cell Longev. 2019;2019:8465030. https://doi.org/10.1155/2019/8465030.

## Publisher's Note